Nanoparticles in a Diblock Copolymer Background: The Potential of Mean Force

Ellen Reister* and Glenn H. Fredrickson

Department of Chemical Engineering and Materials Research Laboratory, University of California, Santa Barbara, California 93106

Received December 5, 2003; Revised Manuscript Received March 31, 2004

ABSTRACT: We have investigated the potential of mean force between two nanoparticles that are surrounded by a symmetric diblock copolymer matrix. The hard nanoparticles are modeled as attractive to one kind of polymer. Using self-consistent-field theory (SCFT), we analyze the energy change of the system when the distance between the particles is changed and subsequently derive the potential of mean force between the particles. Above the order−disorder transition (ODT) the attractive potential of the particles for one kind of monomers leads to a lamellar structure around the particles. These density waves interfere with each other when the distance between the particles is changed, leading to separations with alternating attraction and repulsion between the particles. We further derive analytic results for the potential of mean force in the limit of a weak influence of the particles on the system using the random phase approximation for a diblock copolymer melt. These analytical results are compared with SCFT results. Below the ODT, we insert the particles in such a way that the axis connecting them is either perpendicular or parallel to the lamellar polymer structure. Using SCFT, we study the energy and structural change of the system when the particle distance is changed for these two cases.

1. Introduction

The study of nanoparticles dispersed in polymer backgrounds has become more and more important since unique properties, not held by the polymers or the nanoparticles themselves, may be achieved. Even the addition of low concentrations of particles may have a considerable impact on properties like permeability, tensile modulus, electrical conductivity, catalytic, optical, or magnetic behavior, to name a few.[1−4] These properties usually depend on how the nanoparticles are dispersed in the polymeric system. If the polymer background is composed of copolymers, which generally show a rich phase behavior, the dispersion of the nanoparticles may be controlled in such a way that various nanoparticle patterns are achieved. The mixing of particles with polymers leads to an interesting situation because of the various interactions in the system. The interactions between particles and monomers, between monomers, and the particles themselves can vary widely, depending on the sizes and chemical nature of the particles and polymers. These systems obviously possess a vast parameter space, making them an extremely promising topic to study. However, so far it has only been addressed in a small amount of theoretical work. To create novel materials, it is necessary to have a general understanding on how the order of the polymer background influences the assembly of the particles. On the other hand, the presence of the particles may also influence the morphologies of the polymeric background. Sevink et al.[5] used dynamic density functional theory to study the structure of a diblock copolymer melt with a few immobile particles embedded. Ginzburg et al.[6,7] addressed dynamical properties of systems consisting of nanoparticles and symmetric diblock copolymers by combining cell dynamical systems equations for the polymers and Langevin equations for the particles. A few Monte Carlo simulations of these system have been made by Huh et al.[8] or Wang et al.[9] In recent work Thompson et al.[10] adopted classical self-consistent-field theory (SCFT) calculations to study diblock copolymer systems with embedded nanofillers by incorporating a density functional theory for hard spheres into the field theory underlying SCFT.

SCFT has proved to be a very successful method for analyzing polymeric systems, despite it being a mean-field theory. It describes these systems well because density fluctuations in polymer melts are weak, as long as conditions far away from critical points are considered. Thus, it is natural to consider SCFT as a tool to study polymer systems with inserted particles. One may envisage a combination of particle simulations where the particles are moved according to certain rules, and SCFT is used to compute the forces between particles and relax the surrounding medium. However, SCFT in itself is a numerically fairly elaborate method, making this kind of particle-SCFT simulation computationally expensive. The computational cost could be greatly reduced if the interactions between the particles that are mediated by the surrounding polymers could be expressed by an effective potential. This would allow for simulations of the particles without having to take the polymer background into account explicitly. The quantity that describes the effective interaction between the particles is the potential of mean force. Ginzburg et al.,[11,12] for example, used a combined approach to determine phase diagrams of polymer−clay composites: With SCFT they determined the interaction potential between two infinite, planar surfaces that describe the clay sheets and then used this potential in a density functional theory for finite-sized, rigid clay disks in an incompressible fluid. Groenewold et al.[13] studied the effective interactions between high aspect ratio clay particles in a lamellar copolymer background by calculating the penalty for deforming the lamellar order and analyzed the implications for the stability of the system. Chatterjee et al.[14,15] developed an analytic equation

* Corresponding author. E-mail: reister@mrl.ucsb.edu.

10.1021/ma035849p CCC: $27.50
Published on Web 05/14/2004

theory for treating polymer-induced interactions between colloidal particles and studied their influence on structure and thermodynamics of hard-sphere suspensions.

To provide insight into the potential of mean force between two hard particles in a diblock copolymer background is the main aim of our study. By regarding two particles, we can only deduct pair potentials. If the particle density of the system is high, many-body interactions may not be neglected, but for typical densities of a few weight percent of the particles the pair potential is expected to play the main influence on how the particles assemble. In this paper we consider a symmetric diblock copolymer background and insert two hard particles of diameters between 0.1 and 0.5 radii of gyration R_g of the copolymer. To get an initial understanding, we study the system at temperatures above the order−disorder transition (ODT) so that the potential of mean force is isotropic. The particles are modeled to favor one of the polymer components. We analyze the potential of mean force between the two particles as a function of separation. Below the ODT, when the polymers form a bulk lamellar structure, the potential of mean force is clearly not just a function of separation distance. To investigate this anisotropy, we insert the two particles into an ordered structure such that the line connecting the particles is arranged parallel or perpendicular to the lamellar ordering. The insertion of the particles will cause the lamellae to arrange around the particles. The degree to which the order has to be disturbed when the distance between the particles is altered will determine the energy of the system and will give insight into how the particles would naturally arrange.

To model our system, we develop a field theoretic description that may be used as the starting point for SCFT. With our SCFT calculations we determine the potential of mean force between the particles as a function of distance. Apart from applying the numerical technique of SCFT, we derive a simpler, more approximate analytic expression for the potential of mean force that is also based on a field theoretic description of the system. If the influence of the particles on the system is small, the general expression for the potential of mean force may be expanded, leading to an expression that contains the correlation functions of the effective external fields of the theory. We derive these correlation functions using the classic random phase approximation (RPA). Inserting them into the approximate potential of mean force gives an analytic expression that cannot be solved explicitly but is easily numerically evaluated. To check the validity of these analytical calculations, they are then compared with the SCFT results.

Our paper is arranged in the following way: In the next section we introduce the concept of the potential of mean force, and in section 3 we introduce our model of copolymers and particles and develop a field theoretic description. The following subsections 3.1 and 3.2 elucidate how the potential of mean force using this field theory is calculated in SCFT and analytically using the field correlation functions. The correlation functions are derived in the Appendix. The details of the SCFT calculations are then briefly explained in section 4. Section 5 finally discusses the results of our calculations. By analyzing density profiles, we develop an understanding of the shape of the potential of mean force. In section 5.1, we compare the SCFT results with analytic calculations based on the RPA for temperatures above the ODT. Section 5.2 presents SCFT results for the insertion of particles into a lamellar structure. The paper finishes with some conclusions.

2. Potential of Mean Force

We are interested in the potential of mean force between two particles at positions $\mathbf{R}_1$ and $\mathbf{R}_2$ that are embedded in a polymer background. We assume one particle is fixed at $\mathbf{R}_2 = 0$ and the other may be moved. The average force acting between the two particles may be written as

$$-\left\langle \frac{\partial E}{\partial \mathbf{R}_1} \right\rangle = -\frac{1}{Z}\int \mathscr{D}\{\mathbf{r}\} \frac{\partial E}{\partial \mathbf{R}_1} \exp[-E] \tag{1}$$

where $Z = \int \mathscr{D}\{\mathbf{r}\} \exp[-E]$ is the partition function of the system and the integral $\int \mathscr{D}\{\mathbf{r}\}$ symbolizes the integration over all possible configurational states of the polymer background. The total energy E of the system may be split into two parts E_p and E_0. E_p contains the energy contribution of the particles, i.e., contains all information about position and size of the particles as well as their coupling to the polymers, and E_0 describes the energy of the polymer background without the particles. Equation 1 may be rewritten in the following way:

$$\begin{aligned} -\left\langle \frac{\partial E}{\partial \mathbf{R}_1} \right\rangle = -\left\langle \frac{\partial E_p}{\partial \mathbf{R}_1} \right\rangle &= \frac{1}{Z}\frac{\partial}{\partial \mathbf{R}_1}\int \mathscr{D}\{\mathbf{r}\} \exp[-E_p] \exp[-E_0] \\ &= \frac{1}{Z}\frac{\partial}{\partial \mathbf{R}_1} Z_0 \langle \exp[-E_p]\rangle_0 \\ &= \frac{1}{\langle \exp[-E_p]\rangle_0}\frac{\partial}{\partial \mathbf{R}_1}\langle \exp[-E_p]\rangle_0 \\ &= \frac{\partial}{\partial \mathbf{R}_1} \ln\langle \exp[-E_p]\rangle_0 \end{aligned} \tag{2}$$

$\langle A\rangle_0$ describes the thermodynamic average of A in a system without particles, i.e., for a system with energy E_0 and partition function Z_0. In line three we used the relation $Z = Z_0\langle \exp[-E_p]\rangle_0$ for the partition function of the system. With the last line of eq 2, we may now write down a general expression for the potential of mean force $\mathscr{W}(\mathbf{R}_1,\mathbf{R}_2)$ between two particles at positions $\mathbf{R}_1$ and $\mathbf{R}_2$:

$$\mathscr{W}(\mathbf{R}_1, \mathbf{R}_2) = -\ln\langle \exp[-E_p[\mathbf{R}_1, \mathbf{R}_2, \{\mathbf{r}\}]]\rangle_0 \tag{3}$$

If the polymer background is homogeneous, we may subtract the potential of mean force arising from the insertion of two particles that are so far apart that they are not aware of each other, without changing the physical meaning of $\mathscr{W}$, because $\mathscr{W}(\mathbf{R}_1, \mathbf{R}_2; |\mathbf{R}_1 - \mathbf{R}_2| \to \infty)$ will be constant. If we define $\exp[\epsilon_{p,\infty}] := \langle \exp[-E_p[\mathbf{R}_1, \mathbf{R}_2; |\mathbf{R}_1 - \mathbf{R}_2| \to \infty]]\rangle$ and assume the energy change $E_c = E_p - \epsilon_{p,\infty}$ to be small upon reducing the distance between the particles, $\mathscr{W}(\mathbf{R}_1,\mathbf{R}_2)$ may be expanded in powers of E_c. Expanding to second order leads to the approximate expression:

$$\mathscr{W}(\mathbf{R}_1,\mathbf{R}_2) \approx \langle E_c\rangle_0 - \frac{1}{2}(\langle E_c^2\rangle_0 - \langle E_c\rangle_0^2) \tag{4}$$

3. Field Theory for a Diblock Copolymer System with Inserted Particles

For both the use of self-consistent-field theory and to derive an approximate analytic expression for the

potential of mean force utilizing the random phase approximation (RPA), we need a field theoretic description of the system introduced in this section. We are considering a system of diblock copolymers into which two hard particles are embedded. The particles are modeled to yield an attractive potential for one kind of polymer at their surface. The partition function of this system has the form

$$Z \sim \frac{1}{n!}\int\left(\prod_{i=1}^{n}\mathscr{D}\{\mathbf{r}_{i_A}\}\mathscr{D}\{\mathbf{r}_{i_B}\}\,\mathscr{P}_A[\mathbf{r}_{i_A}]\,\mathscr{P}_B[\mathbf{r}_{i_B}]\right)\times \delta(\hat{\phi}_A+\hat{\phi}_B-1-\delta\Phi_0(\mathbf{r}))\times \exp\left[-\frac{\rho}{N}\int_V \mathrm{d}^3\mathbf{r}\,\{\chi N\hat{\phi}_A\hat{\phi}_B - H(\mathbf{r})(\hat{\phi}_A-\hat{\phi}_B)\}\right] \quad (5)$$

We assume the segment length and segment volume of A and B monomers are identical; N describes the total number of monomers per AB diblock copolymer chain, n the number of copolymers in the system, and ρ the monomer density. $\hat{\phi}_A$ and $\hat{\phi}_B$ denote the microscopic volume fractions of the A and B monomers that are defined through the polymer conformations $\{\mathbf{r}_\alpha(t)\}$:

$$\hat{\phi}_A = \frac{N}{\rho}\sum_{i=1}^{n}\int_0^f \mathrm{d}\tau\,\delta(\mathbf{r}-\mathbf{r}_{i_A}(\tau)) \quad (6)$$

$$\hat{\phi}_B = \frac{N}{\rho}\sum_{i=1}^{n}\int_f^1 \mathrm{d}\tau\,\delta(\mathbf{r}-\mathbf{r}_{i_B}(\tau)) \quad (7)$$

The variable τ, $0 \leqslant \tau \leqslant 1$, parametrizes the contour of the polymer chain, and therefore f describes the average volume fraction of A monomers in the copolymer melt. The different species of monomers interact with each other via the Flory−Huggins parameter χ. The integration $\int\mathscr{D}\{\mathbf{r}_{i_A}\}\mathscr{D}\{\mathbf{r}_{i_B}\}$ is to be understood as the integral over all possible polymer conformations. $\mathscr{P}_A[\mathbf{r}_{i_A}]$ denotes the Gaussian distribution, also called the Wiener measure, of the part of the polymer chain consisting of A monomers, and $\mathscr{P}_B[\mathbf{r}_{i_B}]$ is the equivalent expression for the B monomers:

$$\mathscr{P}_A[\mathbf{r}_A] \sim \exp\left[-\frac{3}{2R_g}\int_0^f \mathrm{d}\tau\left|\frac{\mathrm{d}\mathbf{r}_A}{\mathrm{d}\tau}\right|^2\right] \quad (8)$$

$$\mathscr{P}_B[\mathbf{r}_B] \sim \exp\left[-\frac{3}{2R_g}\int_f^1 \mathrm{d}\tau\left|\frac{\mathrm{d}\mathbf{r}_B}{\mathrm{d}\tau}\right|^2\right] \quad (9)$$

where R_g is the overall radius of gyration of a copolymer chain. The δ-function in eq 5 expresses an incompressibility constraint of the system. We are regarding hard particles in the system that cannot be interpenetrated by the surrounding polymers. Therefore, the overall density of the monomers inside the particles must be zero. This is expressed in the incompressibility constraint through $\delta\Phi_0(\mathbf{r})$, which is -1 inside a particle and 0 otherwise. For one-dimensional (1D) systems $\delta\Phi_0(x)$ takes the form

$$\delta\Phi_0(x) = -\int_{-R/2}^{R/2}[\delta(x+x'-R_1)+\delta(x+x'-R_2)]\,\mathrm{d}x' \quad (10)$$

Real nanoparticle composites are obviously three-dimensional compositions. For computational convenience, however, we restrict our calculations to one and two dimensions. When we speak of 1D systems, we are actually referring to a three-dimensional system with density inhomogeneities only occurring in one direction and the density in the other directions being uniform. Therefore, eq 10 describes a system of two hard parallel slabs of width R and a distance between the centers of the slabs of $|R_1 - R_2|$.

Equivalently, two-dimensional (2D) systems have a plane with nonuniform densities that is uniformly extended into the third dimension. In 2D we assume the "particles" to be square columns with the sides of the cross-sectional area being of length R and the center positions at $\mathbf{R}_1$ and $\mathbf{R}_2$; $\delta\Phi_0(\mathbf{r})$ then takes the form (we impose $R_{1,y} = R_{2,y}$)

$$\delta\Phi_0(\mathbf{r}) = -\int_{-R/2}^{R/2}\mathrm{d}y'\int_{-R/2}^{R/2}\mathrm{d}x'\,\delta(y+y'-R_{1,y})\times [\delta(x+x'-R_{1,x})+\delta(x+x'-R_{2,x})] \quad (11)$$

The attractive interaction energy of the particles with the A monomers (and repulsive interaction with the B monomers) is given by $E_{pm} = -(\rho/N)\int_V \mathrm{d}^3\mathbf{r}\,H(\mathbf{r})(\hat{\phi}_A-\hat{\phi}_B)$. For the following calculations we use a surface interaction of the particles with the surrounding polymers. In 1D we use

$$H_S(x) = h[\delta(|x-R_1|-R/2)+\delta(|x-R_2|-R/2)] \quad (12)$$

If the particles, which we assume to be of length L in the two uniform dimensions, are fully wet by A monomers, this surface interaction leads to an energy decrease of the system by $E_{wet} = -L^2(\rho/N)4h$. It must be noted that the interaction constant h has the dimension of energy times length which may be interpreted as the product of the interaction energy coefficient and an effective interaction length. In 2D systems this surface interaction is given by (imposing $R_{1,y} = R_{2,y}$)

$$H_S(\mathbf{r}) = 2h\{\delta(|y-R_{1,y}|-R/2)\int_{-R/2}^{R/2}\mathrm{d}x'\,[\delta(x+x'-R_{1,x})+\delta(x+x'-R_{2,x})]+[\delta(|x-R_{1,x}|-R/2)+\delta(|x-R_{2,x}|-R/2)]\int_{-R/2}^{R/2}\mathrm{d}y'\,\delta(y+y'-R_{1,y})\} \quad (13)$$

If the two particles are fully wet by A monomers, and the square "columns" are of length L, this gives an energy decrease of $E_{wet} = -L(\rho/N)8hR$. The interpretation of h remains the same as in 1D.

We now develop a field theory from the partition function in eq 5 by performing the common Hubbard−Stratonovich transformation, which leads to the new partition function

$$Z \sim \int\mathscr{D}U\mathscr{D}W\,\exp\{-E[U,W]\} \quad (14)$$

with the new effective Hamiltonian:

$$E[U,W] = \frac{\rho}{N}\int_V \mathrm{d}^3\mathbf{r}\left\{\frac{(H(\mathbf{r})+W(\mathbf{r}))^2}{\chi N}+\frac{\chi N(1+\delta\Phi_0(\mathbf{r}))^2}{4}-U(\mathbf{r})(1+\delta\Phi_0(\mathbf{r}))\right\}-\frac{\rho V}{N}\ln Q[U,W] \quad (15)$$

This result is very similar to the usual result for diblock

copolymer systems.[16] The result is also similar to the result of Thompson et al.;[10] however, in their approach the density of the particles is also transformed into a field because the position of the particles is not fixed in their model. To include the excluded volume of the hard particles, they introduce an additional hard sphere term from a density functional theory by Tarazona[17] that is based on the Carnahan−Starling equation of state[18] for hard spheres. In our model we keep the density of the particles fixed, i.e., do not regard the position of the particles as a degree of freedom and therefore do not transform $\delta\Phi_0$ into a density field and do not have to introduce the excluded-volume penalty term.

U and W are effective fields acting on the polymers: U may be interpreted as a pressure field that ensures the incompressibility constraint and is the conjugate variable to the overall density $\hat{\phi}_A + \hat{\phi}_B$. W is the conjugate variable to the composition $\hat{\phi}_A - \hat{\phi}_B$ and may be interpreted as an exchange chemical potential. $Q[U,W]$ is the partition function of a single polymer chain in the external fields U and W:

$$Q[U,W] = \int \mathcal{D}\{\mathbf{r}_A\}\, \mathcal{D}\{\mathbf{r}_B\}\, \mathcal{P}_A[\mathbf{r}_A]\, \mathcal{P}_B[\mathbf{r}_B] \exp[-\int_0^f \mathrm{d}s\, [U(\mathbf{r}_A(s)) + W(\mathbf{r}_A(s))] - \int_f^1 \mathrm{d}s\, [U(\mathbf{r}_B(s)) - W(\mathbf{r}_B(s))]] \quad (16)$$

The effective Hamiltonian in eq 15 may be split into two contributions $E = E_\mathrm{p} + E_0$. We identify the contribution E_p that contains all information about the particles that have been inserted into the system:

$$E_\mathrm{p}[U, W] = \frac{\rho}{N}\int_V \mathrm{d}^3\mathbf{r} \left\{\frac{H^2}{\chi N} + \frac{2WH}{\chi N} + \frac{\chi N}{4}(2\delta\Phi_0 + \delta\Phi_0{}^2) - U\delta\Phi_0\right\} = \mathrm{const} + \frac{\rho}{N}\int_V \mathrm{d}^3\mathbf{r} \left\{\frac{2H}{\chi N} W - \delta\Phi_0 U\right\} \quad (17)$$

As was expected, the remaining contribution equals the energy of the pure diblock copolymer system:[16,19]

$$E_0[U,W] = -\frac{\rho V}{N} \ln Q[W,U] + \frac{\rho}{N}\int_V \mathrm{d}^3\mathbf{r} \left\{\frac{\chi N}{4} + \frac{W^2}{\chi N} - U\right\} \quad (18)$$

3.1. The Potential of Mean Force in Self-Consistent-Field Theory. The above derivation of a field theory has simplified the original partition function; however, the exact solution of the partition function in eq 14 remains a formidable, if not impossible, task. Self-consistent-field theory introduces a saddle point approximation to the integral in eq 14 that is equivalent to only regarding the largest contribution to the integral. This means that in self-consistent field theory the saddle point of energy $E[U,W]$ with respect to U and W is sought-after, leading to a set of equations that needs to be solved self-consistently. The exact procedure is explained in section 4. The saddle point approximation leads essentially to a mean-field theory of the system. Equation 3 is the general expression for how the potential of mean force between two particles must be calculated. For our field theory this means

$$\mathcal{W}(\mathbf{R}_1,\mathbf{R}_2) = -\ln\left[\frac{\int \mathcal{D}U\mathcal{D}W \exp[-E_0 - E_\mathrm{p}]}{\int \mathcal{D}U\mathcal{D}W \exp[-E_0]}\right] = -\ln\left[\frac{\int \mathcal{D}U\mathcal{D}W \exp[-E]}{\int \mathcal{D}U\mathcal{D}W \exp[-E_0]}\right] \quad (19)$$

In SCFT, instead of calculating thermodynamic averages, the maximal contributions to the integral are used. This leads to the following expression for the potential of mean force:

$$\mathcal{W}(\mathbf{R}_1,\mathbf{R}_2) \approx E^* - E_0^* = E^* + \mathrm{const} \quad (20)$$

Here, E^* is the effective energy at the saddle point of a system with two nanoparticles, and E_0^* is the saddle point energy of a system without the inserted particles. Defining the potential of mean force in such a way that it is zero if the particles are so far apart that they do not interact with each other; this equation tells us that for SCFT it is sufficient to calculate the effective energy of the system. A constant shift of the energy by the calculated energy when the particles are very far apart will reveal the potential of mean force.

3.2. The Potential of Mean Force Using the Random Phase Approximation. If the energy contribution E_p of the particles to the system is small compared to the energy E_0 of the system without particles, the potential of mean force $\mathcal{W}(\mathbf{R}_1,\mathbf{R}_2)$ between the two particles is approximately given by eq 4. Using the particle energy E_p of eq 17, $\mathcal{W}(\mathbf{R}_1,\mathbf{R}_2)$ takes the form (we set $\mathbf{R}_2 = 0$)

$$\mathcal{W}(\mathbf{R}_1) = \mathrm{const} + \frac{\rho}{N}\int_V \mathrm{d}^3\mathbf{r} \left\{\frac{2H(\mathbf{r},\mathbf{R}_1)}{\chi N}\langle W(\mathbf{r})\rangle_0 - \delta\Phi_0(\mathbf{r},\mathbf{R}_1)\langle U(\mathbf{r})\rangle_0\right\} - \frac{1}{2}\left(\frac{\rho}{N}\right)^2 \int_V \mathrm{d}^3\mathbf{r} \int_V \mathrm{d}^3\mathbf{r}' \left\{\delta\Phi_0(\mathbf{r},\mathbf{R}_1)\, \delta\Phi_0(\mathbf{r}',\mathbf{R}_1)\langle \delta U(\mathbf{r})\, \delta U(\mathbf{r}')\rangle_0 - \frac{4H(\mathbf{r},\mathbf{R}_1)\delta\Phi_0(\mathbf{r}',\mathbf{R}_1)}{\chi N}\langle \delta U(\mathbf{r})\, \delta W(\mathbf{r}')\rangle_0 + \frac{4H(\mathbf{r},\mathbf{R}_1)\, H(\mathbf{r}',\mathbf{R}_1)}{(\chi N)^2}\langle \delta W(\mathbf{r})\, \delta W(\mathbf{r}')\rangle_0\right\} \quad (21)$$

where we have used the relations $\delta U = U - \langle U\rangle_0$ and $\delta W = W - \langle W\rangle_0$. To calculate $\mathcal{W}(\mathbf{R}_1)$, we need the correlation functions $\langle \delta W(\mathbf{r})\, \delta W(\mathbf{r}')\rangle_0$, $\langle \delta U(\mathbf{r})\, \delta W(\mathbf{r}')\rangle_0$, and $\langle \delta U(\mathbf{r})\, \delta U(\mathbf{r}')\rangle_0$, which are derived in the Appendix using the standard random phase approximation (RPA) for diblock copolymers.[20,21] Their Fourier transforms are given by

$$\langle \delta W(q)\, \delta W(-q)\rangle_0 = -\frac{1}{D(q)} C_{\mathrm{UU}}(q) \quad (22)$$

$$\langle \delta U(q)\, \delta W(-q)\rangle_0 = -\frac{1}{D(q)} C_{\mathrm{UW}}(q) \quad (23)$$

$$\langle \delta U(q)\, \delta U(-q)\rangle_0 = -\frac{1}{D(q)} C_{\mathrm{WW}}(q) \quad (24)$$

with

$$C_{WW}(q) = -\frac{2}{\chi} + [S_{AA}(q) - 2S_{AB}(q) + S_{BB}(q)] \quad (25)$$

$$C_{UW}(q) = S_{AA}(q) - S_{BB}(q) \quad (26)$$

$$C_{UU}(q) = S_{AA}(q) + 2S_{AB}(q) + S_{BB}(q) \quad (27)$$

$$D(q) = [C_{UU}(q)\, C_{WW}(q) - C_{UW}(q)\, C_{UW}(q)] \quad (28)$$

and

$$S_{AA}(q) = \frac{2N[fx + \exp(-fx) - 1]}{x^2} \quad (29)$$

$$S_{AB}(q) = \frac{N[\exp(-x) - \exp(-fx) - \exp(-(1-f)x) + 1]}{x^2} \quad (30)$$

$$S_{BB}(q) = \frac{2N[(1-f)x + \exp(-(1-f)x) - 1]}{x^2} \quad (31)$$

with the definition $x = q^2/R_g^2$.

Using these correlation functions, we rewrite eq 21 in such a way that the Fourier transforms may be used. For temperatures above the order−disorder transition (ODT), the correlation functions of the fields are a function of the distance $|\mathbf{r} - \mathbf{r}'|$ only. We can therefore use the relation $\int d^3\mathbf{r} \int d^3\mathbf{r}'\, f(\mathbf{r})\, f(\mathbf{r}')\, S(\mathbf{r} - \mathbf{r}') = (2\pi)^{-3} \int d^3\mathbf{q}\, S(\mathbf{q})\, f(\mathbf{q})\, f(-\mathbf{q})$, leading to a simplified expression for the potential of mean force:

$$\mathscr{W}(\mathbf{R}_1) = \text{const} + \frac{1}{2}\frac{1}{8\pi^3}\frac{\rho^2}{N^2}\int d^3\mathbf{q} \left\{\delta\Phi_0(\mathbf{q},\mathbf{R}_1)\delta\Phi_0(-\mathbf{q},\mathbf{R}_1)\frac{C_{WW}(q)}{D(q)} - \frac{4H(\mathbf{q},\mathbf{R}_1)\delta\Phi_0(-\mathbf{q},\mathbf{R}_1)}{\chi N}\frac{C_{UW}(q)}{D(q)} + \frac{4H(\mathbf{q},\mathbf{R}_1)\, H(-\mathbf{q},\mathbf{R}_1)}{(\chi N)^2}\frac{C_{UU}(q)}{D(q)}\right\} \quad (32)$$

Although the previous derivation was performed for three-dimensional systems, it is straightforward to use this expression analogously for one or two-dimensional problems. Formally, only the factor $8\pi^3$ needs to be replaced by $(2\pi)^d$, with d being the dimension of the system, and the dimensionality of the wavevector integrals has to be reduced accordingly.

To calculate the potential of mean force for the particle geometry of eq 10 and particle−polymer interaction of eq 12, we have to calculate the Fourier transforms of $\delta\Phi_0$ and H_S. In 1D these are given by

$$H_S(q) = (1 + e^{-iqR_1})2h\cos(qR/2) \quad (33)$$

and

$$\delta\Phi_0(q) = -(1 + e^{-iqR_1})\frac{2\sin(qR/2)}{q} \quad (34)$$

In 2D they have the form

$$H_S(\mathbf{q}) = (1 + e^{-i\mathbf{q}\mathbf{R}_1})2h\left\{\frac{\cos(q_xR/2)\sin(q_yR/2)}{q_y} + \frac{\cos(q_yR/2)\sin(q_xR/2)}{q_x}\right\} \quad (35)$$

and

$$\delta\Phi_0(\mathbf{q}) = -(1 + e^{-i\mathbf{q}\mathbf{R}_1})\frac{4\sin(q_xR/2)\sin(q_yR/2)}{q_xq_y} \quad (36)$$

if $\mathbf{R}_2 = 0$ is used.

It is not possible to analytically calculate the potential of mean force according to eq 32. However, the numerical evaluation is straightforward. Results of these numerical calculations are presented in section 5.

4. Self-Consistent-Field Theory Calculations

With eqs 14 and 15 we have a field theoretic description of the system. As mentioned in section 3.1, SCFT is equivalent to the saddle point of the effective Hamiltonian 15 with respect to U and W. The resulting equations are

$$\frac{\delta E}{\delta W} = 0\Big|_{u,w}: \ \phi_A^*(\mathbf{r}) - \phi_B^*(\mathbf{r}) = -\frac{2(H(\mathbf{r}) + w(\mathbf{r}))}{\chi N} \quad (37)$$

$$\frac{\delta E}{\delta U} = 0\Big|_{u,w}: \ \phi_A^*(\mathbf{r}) + \phi_B^*(\mathbf{r}) = 1 + \delta\Phi_0(\mathbf{r}) \quad (38)$$

where we have used the definitions

$$\phi_A^*(\mathbf{r}) = -\frac{1}{Q[U,\,W]}\frac{\delta Q[U,\,W]}{\delta(U+W)}\Big|_{u,w} \quad (39)$$

$$\phi_B^*(\mathbf{r}) = -\frac{1}{Q[U,\,W]}\frac{\delta Q[U,\,W]}{\delta(U-W)}\Big|_{u,w} \quad (40)$$

From these definitions, we see that $\phi_A^*(\mathbf{r})$ and $\phi_B^*(\mathbf{r})$ are the average densities of A and B monomers in the external fields $u + w$ and $u - w$. Lower case letters u and w denote the saddle point fields corresponding to U and W, respectively.

Using a path-integral formulation to describe polymer chains,[22,23] the single-chain partition function and the densities of the polymers may be explicitly calculated: We introduce the propagator $q(\mathbf{r},t)$ that describes the probability to find the end of a polymer chain of length t ($0 \leq t \leq 1$) with the constraint that the monomer at t is of species A, if $t \leq f$, and of species B otherwise.[19]

$$q(\mathbf{r},t) = \int \mathscr{D}\{\mathbf{r}_A\} \int \mathscr{D}\{\mathbf{r}_B\}\, \mathscr{P}_A[\mathbf{r}]\, \mathscr{P}_B[\mathbf{r}]\, \delta(\mathbf{r} - \mathbf{r}(t)) \exp[-\int_0^t ds\, [\Theta(f-s)(U(\mathbf{r}(s)) + W(\mathbf{r}(s))) + (1 - \Theta(f-s))(U(\mathbf{r}(s)) - W(\mathbf{r}(s)))]] \quad (41)$$

$\Theta(t)$ is the Heaviside function, which is 1 for $t > 0$ and 0 otherwise. Analogously, we introduce the propagator $q^\dagger(\mathbf{r},t)$ with the same interpretation apart from the constraint that the end monomer has to be of species B if $t \leq (1 - f)$ and of A otherwise. If the copolymers are

subject to the external potentials U and W, the following differential equations hold for these propagators:

$$\frac{\partial q(\mathbf{r},t)}{\partial t} = \begin{cases} R_g^2\nabla^2 q(\mathbf{r},t) - (U+W)q(\mathbf{r},t) & \text{if } 0 \leqslant t \leqslant f \\ R_g^2\nabla^2 q(\mathbf{r},t) - (U-W)q(\mathbf{r},t) & \text{if } f < t \leqslant 1 \end{cases} \tag{42}$$

$$\frac{\partial q^\dagger(\mathbf{r},t)}{\partial t} = \begin{cases} R_g^2\nabla^2 q^\dagger(\mathbf{r},t) - (U-W)q^\dagger(\mathbf{r},t) & \text{if } 0 \leqslant t \leqslant 1-f \\ R_g^2\nabla^2 q^\dagger(\mathbf{r},t) - (U+W)q^\dagger(\mathbf{r},t) & \text{if } 1-f < t \leqslant 1 \end{cases} \tag{43}$$

with the initial condition $q(\mathbf{r}, t=0) = q^\dagger(\mathbf{r}, t=0) = 1 + \delta\Phi_0(\mathbf{r})$. The solution of these partial differential equations gives us the possibility to calculate the single-chain partition function Q and the number densities of the A and B monomers. The relation

$$Q[U,W] = \int_V \mathrm{d}^3\mathbf{r}\; q(\mathbf{r}, t=1) \tag{44}$$

provides a route to compute Q. The monomer densities are calculated using these equations:

$$\phi_A(\mathbf{r}) = \frac{1}{Q}\int_0^f \mathrm{d}t\; q(\mathbf{r}, t)\, q^\dagger(\mathbf{r}, 1-t) \tag{45}$$

$$\phi_B(\mathbf{r}) = \frac{1}{Q}\int_f^1 \mathrm{d}t\; q(\mathbf{r}, t)\, q^\dagger(\mathbf{r}, 1-t) \tag{46}$$

The numerical SCFT calculations are performed in real space on an equidistant lattice in 1D and a square lattice in 2D with periodic boundary conditions. While the realization of $\delta\Phi_0(\mathbf{r})$ on the lattice is straightforward, the interaction potential of the particles with the monomers has to be carefully regarded. In 1D we assume the potential $H_S(x)$ only acts on the two neighboring lattice sites on either side of a particle. We set the strength of the potential to $H_{nn} = h/\mathrm{d}x$, with dx being the lattice spacing. The total energy added to the system when both particles are fully wet by A monomers is $E_{\mathrm{wet}} = -L^2(\rho/N)4h$ (again assuming the system is of length L in the two homogeneous directions). In a 2D system the potential also only acts on the neighboring lattice sites that are one lattice site away from the particle and is set to $H_{nn} = 4hR/(N_H\,\mathrm{d}x\,\mathrm{d}y)$. d$x$ and dy are the lattice spacings in the x- and y-directions, and N_H is the number of lattice sites where the potential acts. The added energy of two totally wet particles is $E_{\mathrm{wet}} = -L(\rho/N)8hR$, if the length of the system is L in the third dimension. When comparing the previously introduced RPA calculations with the SCFT results, the particle size and the energy E_{wet} should be matched.

In SCFT we initially start with random fields U and W at each lattice site. Adding homogeneous contributions to U and W does not change the physics of the system. Therefore, we impose that $\int_V \mathrm{d}^3\mathbf{r}\; U(\mathbf{r}) = \int_V \mathrm{d}^3\mathbf{r}\; W(\mathbf{r}) = 0$ at all times. With these fields we solve the diffusion equations (42) and (43) utilizing pseudospectral methods.[24] The propagators q and $q^\dagger$ provide access to the single-chain partition function and the densities for the given fields. To find a solution of the saddle point eqs 37 and 38, we employ the dynamic equations[25,26]

$$\frac{\partial U(\mathbf{r},\tau)}{\partial \tau} = \lambda\,\frac{\delta E[U,W;\tau]}{\delta U} = \lambda[\phi_A(\mathbf{r},\tau) + \phi_B(\mathbf{r},\tau) - 1 - \delta\Phi_0(\mathbf{r})]$$

$$\frac{\partial W(\mathbf{r},\tau)}{\partial \tau} = -\lambda\,\frac{\delta E[U,W;\tau]}{\delta W} = -\lambda\left[\phi_A(\mathbf{r},\tau) - \phi_B(\mathbf{r},\tau) + 2\,\frac{W(\mathbf{r},\tau) + H(\mathbf{r})}{\chi N}\right] \tag{47}$$

τ may be interpreted as a "time" and λ as a "diffusion constant"; however, the nonconserved relaxational dynamics of these equations should not be mistaken for realistic polymer dynamics. These dynamic equations should rather be regarded as a tool with which the system is relaxed to the saddle point solution we are interested in. After finding the densities for the given fields, the right-hand side of eqs 47 are evaluated. The new fields after a discrete "time step" $\delta\tau$ are then given through $U(\tau + \delta\tau) = U(\tau) + \lambda(\delta E[U,W;\tau]/\delta U)\delta\tau$, and similarly for the field W. We then calculate the densities given by the new fields and repeat the whole procedure until a certain desired tolerance in the dynamical equations has been reached.

5. Results

In our study we aim to develop a general understanding of the potential of mean force between two particles attracting one kind of monomer in a diblock copolymer background and check the validity of the approximate expression for $\mathscr{W}(R_1)$ of eq 32 by comparing with SCFT results. We are further interested in how the insertion of particles into an ordered polymer background influences the system.

5.1. Potential of Mean Force in RPA and the Comparison with SCFT. In this section we present SCFT results and numerical results based on eq 32. Because eq 32 cannot be explicitly evaluated, we compute the potential of mean force $\mathscr{W}(R_1)$ numerically using a simple trapezoidal rule for the integral and setting a cutoff in the wave vector where the integrand is small enough. However, a few aspects of the numerical integration have to be elucidated. The correlation function $\langle\delta W(q)\,\delta W(q)\rangle$ approaches the constant $\chi N/2$ for large wave vectors, and $\langle\delta U(q)\,\delta U(q)\rangle$ has an asymptotic behavior of $2\chi N(f - {}^1/_2)^2 - (1+q^2)/2$ in the limit $q \to \pm\infty$. If we regard the integrand of eq 32, we see that in the limits $q \to \pm\infty$ it does not decrease to zero, and therefore the integral will diverge. One of the reasons for the divergence is for example that the regarded overall density profile drops discontinuously from 1 to 0 at the surface of the particles. Using a more realistic continuous density profile can overcome the divergence of the integral term proportional to $\langle\delta U(q)\,\delta U(q)\rangle$. However, the results of test calculations with a continuous density profile coincided with those using eq 10 because our calculation probes the energy change when the particles are moved and not the energy of the particle−polymer interface. In general, the divergence of eq 32 can be eliminated by adding a function $g(\mathbf{q},R_1)$ to the integrand. The physics of the problem will not be changed as long as the integral $\int \mathrm{d}^3\mathbf{q}\; g(\mathbf{q},R_1)$ is independent of R_1. For all contributions to eq 32, appropriate functions that meet these requirements can

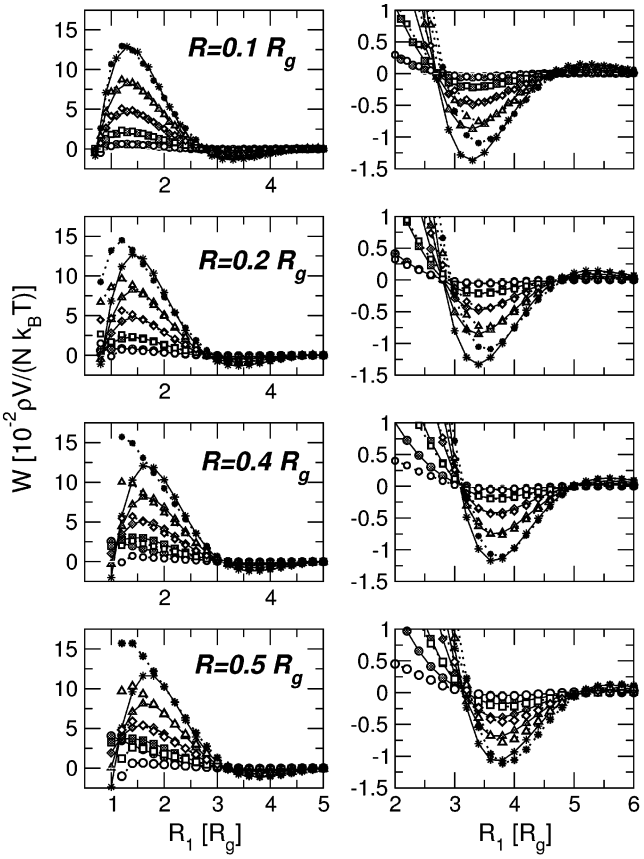

Figure 1. Comparison of the potential of mean force resulting from SCFT with that resulting from the analytic expression of eq 32 using the surface potential H_S for 1D systems. The system size in SCFT is $35R_g$ with a lattice spacing of dx = 0.1. Each row of plots is for the given particle size R. Solid lines with shaded symbols follow from the analytic calculations and dashed lines with white symbols from SCFT. The different interactions h = 0.1, 0.2, 0.3, 0.4, and 0.5 are symbolized through the circles, squares, diamonds, triangles, and stars, respectively. Panels on the left highlight the region where $\mathscr{W}(R_1)$ is positive those on the right where $\mathscr{W}$ is negative. The agreement diminishes for increasing particle size and interaction strength for small distances. For larger distances the agreement stays better.

be found. The numerical integrations were performed within the limits $-40/R_g < q_i < 40/R_g$. Larger intervals were explored without significant changes in the results.

In Figure 1, we have plotted the potentials of mean force as a function of interparticle distance R_1 for different sizes of the particles and different strengths of the particle−polymer interaction in a 1D system with the left panel highlighting the region of a positive potential and the right panels the first negative region. Each row of graphs represents a different particle size, and every line in a graph corresponds to a given parameter h. Solid lines with shaded symbols result from using our proposed surface potential $H_S(\mathbf{r})$ (cf. eq 12), and dashed lines with white symbols follow from SCFT calculations. The parameters of this figure are $\chi N = 6$ and $f = 0.5$.

The plots reveal an oscillating potential that is strongly damped with increasing particle distance. For small distances the potential has a strong positive peak, expressing a strong attraction between the particles before the maximum is reached. Upon increasing the distance the particles repel each other. The repulsion becomes weaker until at some point the potential reaches a minimum at approximately $3.2R_g$. If the particles are moved even further apart, the potential increases, again implying an attractive force between the particles. The potential grows until a weak maximum is reached. For large distances the potential finally reaches a constant, where the particles do not feel each other anymore. The oscillating behavior of the potential is understandable by regarding the density profiles around the particles. The insertion of one particle into the system that attracts A monomers into the copolymer background above the ODT will create some structure around the particle. We expect an enrichment of the A monomers near the surface of the particle; further away a depletion layer of A, i.e., an enrichment layer of B, will appear. If the particle−polymer interaction is strong, even further away from the particle a weak increase in the A density will be visible due to polymers containing an A and a B block. Even though the temperature is above the ODT, the particle creates a lamellar structure with the amplitude of the oscillatory density profile decreasing with increasing distance from the particle. For the one-dimensional system, where the particle actually represents a hard slab with width R, the density profile near the particle resulting from SCFT calculations is represented in Figure 2 for $\chi N = 6$, f = 0.5, h = 0.3, and $R = 0.2R_g$. We observe exactly the expected behavior: the particle is wet by A monomers leading to a surrounding lamellar structure with the amplitude decreasing with distance.

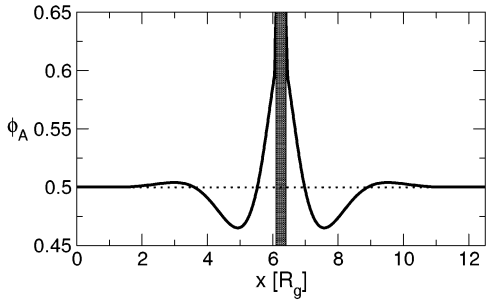

Figure 2. Density profile of A monomers caused by the insertion of one particle with $R = 0.2R_g$ into a symmetric diblock copolymer background with $\chi N = 6$. The interaction strength between polymers and particle is $h = 0.3$.

If we now insert two particles into the system, the created "density waves" outside the particles will interfere with each other. Using Figure 2, imagine we have two particles that create the same kind of density profile. The first minimum of the A density, or the first maximum of the B density, is approximately $1R_g$ away from the first particle. If we now insert the second particle that would energetically prefer to be wet by A monomers about $1R_g$ away from the other particle, this will be energetically very unfavorable for the system. This is expressed by the first maximum of the potential of mean force in the plots of Figure 1. However, if we have a distance of about $3R_g$ between the particles, the density maximum of one particle will coincide with the next-nearest density maximum of the other particle. This is obviously energetically favorable, which we see as a minimum in the potential of mean force. At a distance of approximately $4R_g$ from a particle the density equals the equilibrium value of a system without particles, and therefore at distances between the particles larger than about $8R_g$ the first particle is not aware of another particle leading to a constant potential of mean force. The actual profiles for systems with two

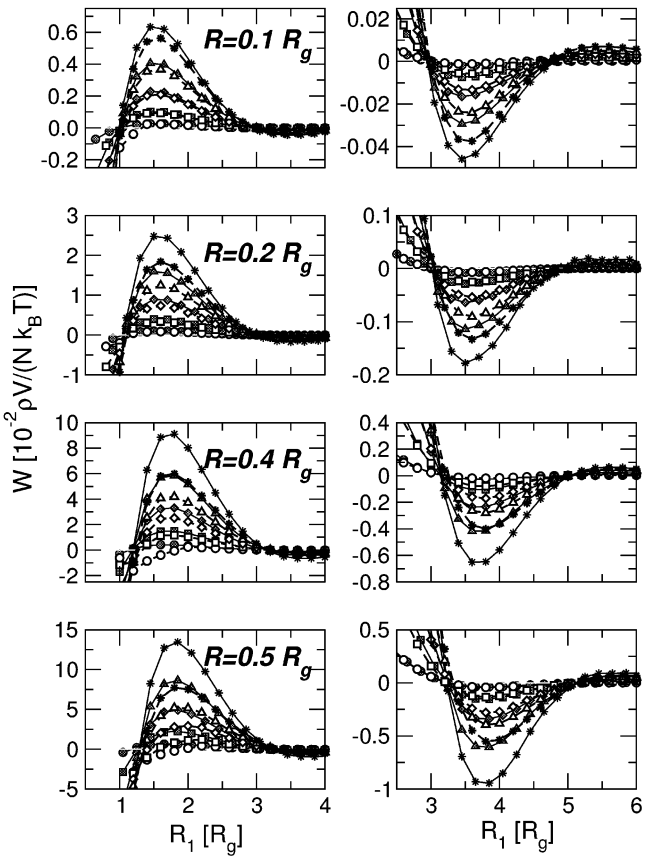

Figure 3. Corresponding plot to Figure 1 but now for 2D systems. The interaction strengths $h = 0.2$, 0.4, 0.6, 0.8, and 1.0 are symbolized through the circles, squares, diamonds, triangles, and stars, respectively. The system size in SCFT is $16R_g \times 8R_g$ with a lattice spacing of $dx = dy = 0.1R_g$. Qualitatively good agreement is achieved, but as expected increasing h and particle size leads to quantitative disagreement.

particles are shown in Figure 4 and will be discussed during the comparison of RPA and SCFT.

The analogous results to Figure 1 for 2D systems are displayed in Figure 3, also for $\chi N = 6$ and $f = 0.5$. Comparing the results of the 2D system with those for 1D, we qualitatively find the same damped oscillating behavior of $\mathscr{W}$. In the 1D case we saw that the increase in particle size only changes the amplitude very weakly. In the 2D systems, however, the amplitude strongly increases with increasing particle size. The reason for this is that the increased particle size does not only increase the contribution to $\mathscr{W}$ caused by $\delta\Phi_0$, but also the potential $H_S(\mathbf{r})$ is significantly changed.

We now focus on the comparison of the potential of mean force achieved by SCFT and analytic calculations. In SCFT we have to use a finite system size for the calculations. Because of the periodic boundary conditions employed, interactions between the particles are not limited to the interactions inside the system size but may also appear between the particles in the simulation box and the replicas of the particles generated by the boundary conditions. In Figure 1 we see that the interaction between the particles becomes negligible for distances greater than approximately $8R_g$. In other words, the system size used in SCFT must be at least $8R_g$ larger in extension than the maximum distance between the particles regarded. The 1D calculations shown in this section were performed using a system size of $35R_g$. In 2D we set the system size to $16R_g \times$

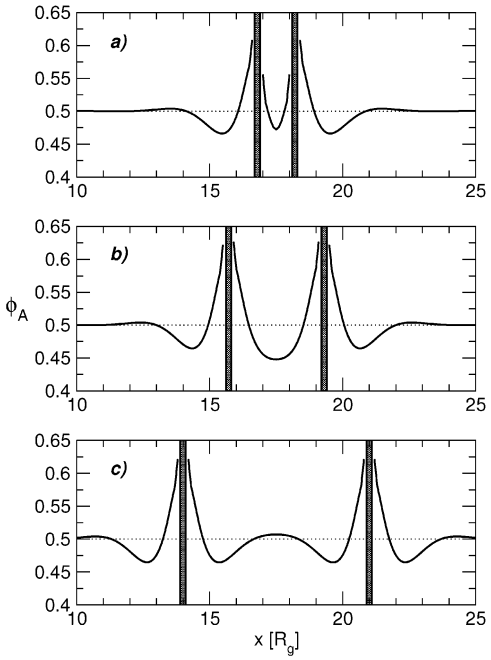

Figure 4. Density profiles of 1D systems with two inserted particles of size $R = 0.2$ and $h = 0.3$. The three chosen distances, $R_1 = 1.4$, 3.6, $7R_g$, correspond to the first maximum, the first minimum of the potential of mean force, and a negligible potential.

$8R_g$. The lattice spacing in both cases is $dx = dy = 0.1R_g$. Studying Figure 1, we in general find that qualitatively SCFT results in the same expected behavior as the RPA estimate, namely a potential of mean force oscillating and damped with increasing distance between the particles. Even quantitatively good agreement is achieved. However, it must be noted that visibly good agreement is only achieved by shifting the analytic results along the axis denoting the particle distance. For $R = 0.1R_g$ we shift by $0.1R_g$, for $R = 0.2R_g$ by $0.2R_g$, for $R = 0.4R_g$ by $0.4R_g$, and for $R = 0.5R_g$ by $0.4R_g$. In the analytic model the surface of the particle coincides with the place where the surface potential of the particle acts on the monomers. On the lattice used in SCFT calculations this obviously cannot be exactly the case, and therefore the size of the particles and the distance between them are slightly displaced. We studied the influence of this effect in 1D systems by using different lattice discretizations and found that the larger the lattice spacing, the more the potential is shifted toward larger R_1. The shifts used in Figure 1, though, cannot be solely explained by this effect. Regarding the smallest particle with $R = 0.1R_g$, we see for weak particle−polymer interaction strengths a very good agreement for distances where the potential is positive. If we regard the distances where the potential becomes negative (cf. the top right panel of Figure 1), the agreement is not quite as good; only for the smallest h the agreement stays as good, and for larger h the analytical results become more negative. Upon increasing the particle size we see for $R = 0.2R_g$ that the behavior at small distances is significantly different: SCFT produces peaks that are shifted to smaller distances, and the heights of the peaks are also bigger than for the analytic calculations. This effect is more pronounced the bigger h is. For $R_1 > 1.4R_g$, however, the decrease of the potential agrees very well for all regarded values of h. The region where $\mathscr{W}$ becomes negative (see right panel) surprisingly agrees better for the bigger particle: only

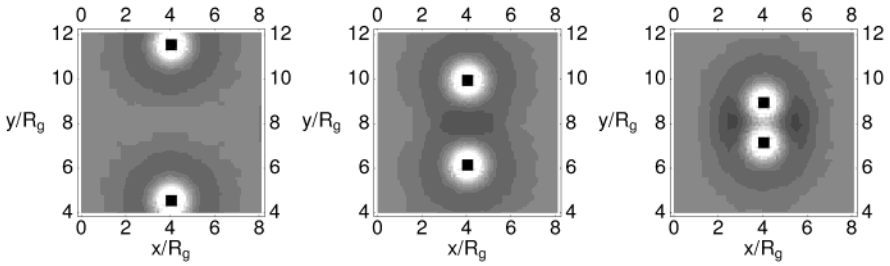

Figure 5. Density plots of the 2D system with two inserted particles. The particle size is $R = 0.4R_g$ and the interaction strength $h = 0.8$. The three displayed distances $R_1 = 7.0R_g$, $3.8R_g$, and $1.8R_g$ correspond analogously to Figure 4 with the first maximum, the first minimum of the potential of mean force, and a position where the potential is negligible. The attraction of *A* monomers to the particles lead to a circular lamellar structure damped with distance around the particle. The "interference" of these "density waves" leads to the observed potential of mean force.

for $h = 0.4$ and $h = 0.5$ do the analytic results become more negative than for SCFT.

Increasing the particle sizes further confirms these trends: SCFT leads to peaks at smaller distances that overestimate the analytical result. The decline of $\mathscr{W}$ for $R > 1.4R_g$ agrees well for the larger *h* values. The right panels show that the analytical calculations and SCFT lead to a quantitative agreement in the region where $\mathscr{W}$ becomes negative for $R = 0.4R_g$ and $0.5R_g$.

Since we previously explained the origin of the oscillating behavior of the potential of mean force, we now look at how the density profiles actually change with increasing the interparticle distance. Figure 4 displays the density profiles around the particles for different distances. The profiles result from SCFT calculations for a system with particle size $R = 0.2R_g$ and $h = 0.3$. Figure 4a is the density profile for two particles with distance $R_1 = 1.4R_g$, which corresponds to the distance where the potential of mean force has its maximum. Examining the density profile between the particles explains why the energy is increased: The particles energetically favor being wet by *A* monomers as can be seen on the other side of the particles. Between the particles, however, the interference of the density profiles around each particle leads to a strong decrease of the *A* density in this region. The enrichment is strongly suppressed, resulting in an increase in energy of the system. If we now analyze the profile between the particles for $R_1 = 3.6R_g$ (see Figure 4b), the situation is the opposite. The enrichment of the particles is increased, which is indicated by both the slight increase in density close to the particle and the widening of the enrichment layer. Furthermore, any gradient in the density profile costs energy because interfacial tension is created. The density minima created by the particles coalesce at this distance removing the part of the profile, where the density increases again. These two effects lead to an energy gain and therefore to a minimum in the potential of mean force. At $R_1 = 7R_g$ (Figure 4c), the density profile between the particles is only altered in the middle. The enrichment layer and the subsequent depletion layers are not influenced by the profiles caused by the other particles. The weak interferences in the middle between the particles leads to a negligible energy change of the system, and therefore the potential of mean force has already reached the value of no interaction between the particles.

We now turn to Figure 3, which is the analogue plot to Figure 1 but for the 2D system. The analytic results have again been shifted along the R_1-axis for the comparison. All solid lines with gray symbols (analytic results) have been shifted by *R*. By looking at the two top panels of Figure 3 for the smallest particle with $R = 0.1R_g$, we find very good qualitative agreement for all distances: for small distances the potential is negative and strongly increases for larger R_1 until a maximum is reached. The position of all maxima coincides very well. The potential then decreases less strongly now, until a negative minimum is reached. Again the position of the minimum coincides very well for all regarded *h*. Quantitatively, the agreement of SCFT and the analytic calculations is very good for the small $h = 0.2$ and becomes less good upon increasing *h*, although for $R = 0.1R_g$ even with $h = 1.0$ a reasonably good quantitative agreement is found. Increasing the particle size still leads to a good qualitative match in the shape of the curves; however, the analytic calculations overestimate the SCFT results by an amount that increases with particle size and particle−polymer interaction. Approaching small distances for the particles with $R = 0.4R_g$ and $0.5R_g$ and $h = 0.2$ and 0.4, the potential of mean force decreases faster in SCFT than in the analytical calculation. This corresponds to observations made in the 1D systems.

Finally, we study the density profiles of the 2D system for different distances between the particles. The densities as a function of separation are displayed in Figure 5 for the particle size $R = 0.4R_g$ and an interaction strength of $h = 0.8$. The plots are for the distances $R_1 = 7.0R_g$, $R_1 = 3.8R_g$, and $R_1 = 1.8R_g$, which correspond respectively to the situation where the particles do not interact with each other, the first minimum, and the first maximum of the potential of mean force. The general findings are similar to the 1D case. For the large distance in the left panel we find an enrichment of *A* monomers at the surface of the particles visible through the white ring around the particle. The next layer around the particles is then depleted of *A* monomers indicated by the darker ring. Further out a homogeneous gray shading shows the density of $\phi_A = 0.5$. Between the two particles the region with $\phi_A = 0.5$ is large, and therefore no interaction between the particles occurs, which is what we see as a flat potential of mean force. When the particles are moved closer together (cf. the center panel of Figure 5) to $R_1 = 3.8R_g$, the density between the particles is below $\phi_A = 0.5$, as was also observed in Figure 4 for the 1D case. The merging of the density minima outside the particles leads to an energy reduction that is visible as a negative potential of mean force in Figure 3. For the distance $R_1 = 1.8R_g$ in the right panel of Figure 5, we see that the density in the middle between the particles is considerably smaller than at the surface. Because the distance is so small, this is only possible through strong gradients of the density profile. Strong gradients in density profiles lead to an increase in energy of the system, which

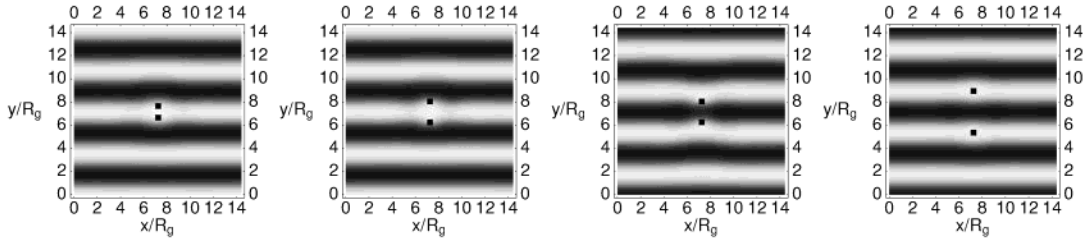

Figure 6. Density of the A monomers when two hard particles with $R = 0.4R_g$ are inserted into a lamellar ordered diblock system with $\chi N = 13$ and $f = 0.5$. The two center panels correspond to the situation where it is energetically same whether the center lamella is of the A or B species. The right panel relates to the energy minimum when the particles are in the center of the A lamellae.

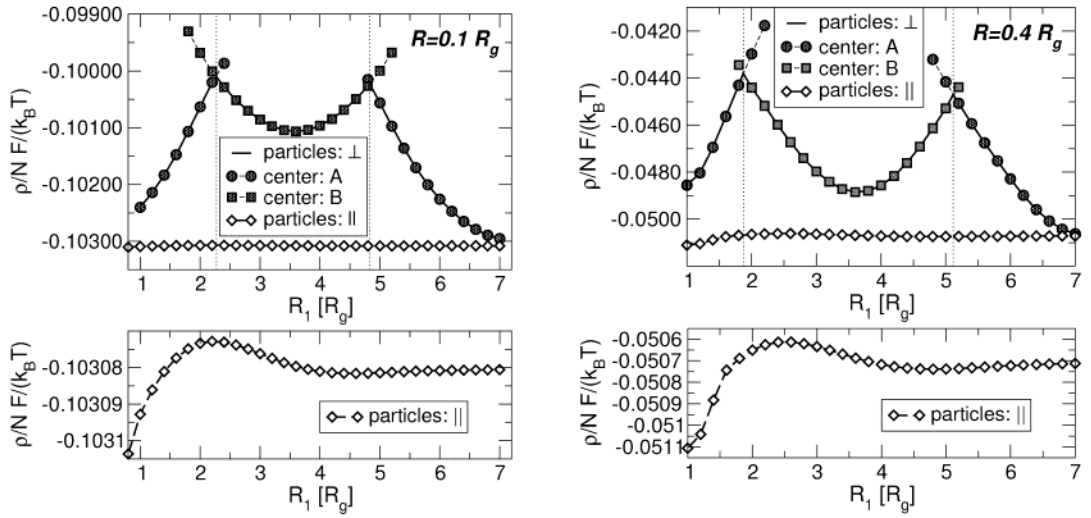

Figure 7. Top panels show the energy of the system as a function of particle distance for the two situations that the particles are inserted in parallel or perpendicular to the polymer structure for the two studied particle sizes: $R = 0.1R_g$ (left) and $R = 0.4R_g$ (right). The bottom panels highlight the energy when the particles are arranged in parallel to the order. The behavior is comparable to that observed in the homogeneous systems.

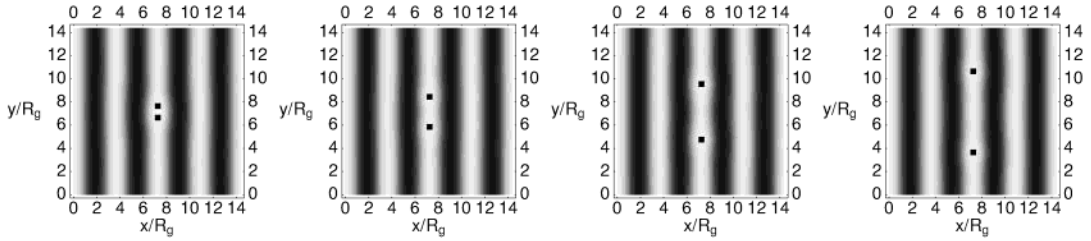

Figure 8. Corresponding plots to Figure 6, but now for particles inserted parallel to the lamellar structure. The panels from left to right correspond to a small particle distance, when only one indent in the lamellar is needed, the distance of the first maximum of the potential of mean force, the distance of the next minimum, and the distance when the particles almost negligibly interact with each other.

explains the positive potential of mean force for small distances.

5.2. Potential of Mean Force below the ODT. So far, our SCFT calculations have been restricted to temperatures above the ODT. Below the ODT, when the copolymer system orders, the potential of mean force will no longer be a simple function of distance between the particles. For example, the angle of the axis connecting the two particles relative to the structure of the polymer system will also become important. Various mechanisms will contribute to the behavior of this system: the particle−polymer interaction leads to an energy decrease when the particle is wet by A monomers; however, the presence of a particle near the interface between an A- and a B-lamella possibly reduces the interfacial tension. Finally, the particle may also deform the interfaces between the lamella which will increase the energy. To analyze this interplay and observe how the structure of the system changes with particle distance, we look at two situations: first, the axis connecting the particles is perpendicular to the initial structure and, second, parallel to the lamellae. For the polymer system we use $\chi N = 13$ and $f = 0.5$, the system size is $14.3R_g \times 14.3R_g$. (The length of the system is a multiple of the natural lamellar spacing to ensure that lamellae are formed parallel to the lattice.) The particle sizes regarded are $R = 0.1R_g$ and $R = 0.4R_g$; the interaction strength between polymer and particle is $h = 0.6$.

In Figures 6 and 8 , we show the density profiles at certain separations only for particles of size $R = 0.4R_g$. If the axis connecting the two particles is perpendicular to the lamellar structure (see Figure 6), for small distances the lamella extends around the particle. For the smaller particles (not shown), the structure is only weakly influenced by the particles. Upon increasing the

distance between the particles, the interface between the *A* and *B* monomers is more strongly deformed by the particles. The thick solid line in the top panels of Figure 7 shows the energy of the system as a function of distance when the particles are arranged perpendicular to the structure for $R = 0.1R_g$ (left panel) and $R = 0.4R_g$ (right panel). We clearly see that the increase in distance leads to an increase in energy as was to be expected. When the particle distance is further increased to about $2.2R_g$ for $R = 0.1R_g$ or to about $1.9R_g$ for $R = 0.4R_g$, it is energetically the same whether the particles are both in the center *A* lamella or in the two *A* lamellae adjoining a center *B* lamella. This situation corresponds to the two center panels in Figure 6. For larger distances the latter configuration becomes more favorable. (The dashed lines of Figure 7 with circles represent the free energy when the *A* lamella remains in the center.) When the particles are moved further into the center of the layers, the energy decreases until the minimum is reached at $R_1 = 3.6R_g$. The right panel of Figure 6 shows that the energy minimum results from the particles being situated in the middle of the *A* lamellae. Shifting the particles toward the next *A*−*B* interface increases the energy until at approximately $R_1 = 4.8R_g$ for the smaller particles and $R_1 = 5.1R_g$ for the bigger particles the polymer structure with the *A* lamella in the center again becomes energetically favorable. This kind of behavior will continue further upon increasing particle distance. In Figure 7 we see this periodic behavior in the energy of the system. Only for small separations is this periodic pattern enhanced because the deformed interfaces between *A* and *B* interact with each other.

Figure 8 shows the polymer density at different distances of the particles if the axis connecting the particles is parallel to the lamellar structure. Because the particles are smaller than the lamellar spacing, the structure is influenced only weakly. Nevertheless, because of the presence of the particles, the interface between *A* and *B* has to bulge around the particles. This will be more pronounced for the bigger particles. For small separations one "big" bulge is formed, leading to a lower energy than for larger distances when two indents in the lamellae are formed. This is seen in the bottom panels of Figure 7. However, when the particle distance is increased, the study of the energy reveals a comparable behavior to that found for two particles inserted into a homogeneous background. Along the axis parallel to the particles the density is almost homogeneous, but now the average *A* density is approximately $\phi_A = 0.9$. In principle, the same damped oscillating potential of mean force between the particles should be observed for this density, but with a strongly decreased amplitude. This is exactly what we observe in the lower panels of Figure 7. The surface energy of the bigger particles being so much larger than for the small particles explains why this effect is weaker for the small particles. Overall, the energy of the system when the particle distance parallel to the lamellae is increased is influenced by two factors: (i) the deformation of the *A*−*B* interface around the particles and (ii) the potential of mean force between the particles in the almost homogeneous lamella.

6. Conclusions

In this paper we have developed a field theoretical description of a system consisting of diblock copolymers with two inserted hard particles. We use this description as a starting point to perform SCFT calculations and to develop an approximate analytic expression for the potential of mean force between the particles that makes use of correlation functions derived through RPA. Because of the mean-field character of SCFT, our calculations yield the potential of mean force for a system where fluctuations of the polymer densities are neglected. The analytic expression developed in this study follows from an expansion of the general expression for the potential of mean force to second order in the energy E_p describing the particle−polymer interaction. It is therefore only valid for small particles and weak interactions between the particles and the surrounding copolymers.

Using SCFT and the analytic expression, we explore the general features of the potential of mean force in a system above the ODT of the copolymers. The particles are modeled in such a way that an enrichment of *A* monomers near the particles is energetically favorable through a short-ranged potential. We find that attraction and repulsion between the particles alternate with increasing distance between the particles. The strength of these forces decreases for larger distances. Although we are above the ODT and the imposed particle−polymer interaction is short-ranged, we find that the interparticle interaction is long-ranged, the interaction length being on the order of several radii of gyration. Insight on how this comes about is given by the study of the density profiles around the particles. The interaction of the particle with the polymers leads to a lamellar structure around the particles with decreasing amplitude. We show that the interference of these "density waves" reproduces the observed behavior of the potential of mean force.

To understand the general features of the potential of mean force, we studied the validity of the analytic expression by comparing it with SCFT calculations. For all regarded particle sizes and particle−polymer interaction strengths, the qualitative behavior is the same. Quantitatively good agreement is found for small particles and weak interactions at all distances in both 1D and 2D. If *h* and *R* are increased, quantitative agreement may only be found for certain ranges of distance until no agreement is observed. In general, the divergence of the two theoretical approaches was to be expected, but even for larger particles and stronger interactions the analytic expression still leads to reasonably good qualitative agreement.

After studying the potential of mean force for temperatures above the ODT, we inserted two particles into an initially lamellar ordered structure. For particles arranged perpendicular to the structure, we find a periodic energy of the system with increasing distance depending on how the lamellae can arrange. If the distance between the particles is a multiple of the lamellar spacing, the particles can arrange in the middle of the *A* layer and the energy of the system is at a minimum. For other distances particles have to be moved toward the interface, always leading to an increase in energy. If the particles are inserted parallel to the layering the energy, differences are weak compared to the energy changes when the particles are inserted perpendicular. The behavior is similar to the potential of mean force in disordered systems because the lamella appears almost homogeneous for the particles.

We have only studied the situations in which the axis connecting the two particles is arranged parallel and perpendicular to the initial lamellar structure. But even this shows that in an ordered system the potential of mean force has to be regarded carefully because it is highly anisotropic and depends on how the particles are placed into the structure. Depending on particle size and the interaction strength between particles and polymers, the insertion of particles may actually cause more interesting effects like altering the equilibrium structures of the polymers, possibly leading to other macroscopic properties of the material. In this study we have shown that SCFT may be used as a tool to study polymer systems with particle inclusions. After this initial study we propose to use SCFT as a tool to examine these more complicated systems that yield a rich variety of mesoscopic structures.

Acknowledgment. The authors are grateful to the General Electric Corporate R&D for supporting this work through the Complex Fluids Design Consortium at UCSB. Partial support was also received from the National Science Foundation under DMR03-12097. This work made use of MRL Central Computing Facilities supported by the MRSEC Program of the National Science Foundation under Award DMR00-80034. E.R. acknowledges support from the Deutsche Forschungsgemeinschaft.

Appendix. Calculation of the Field Correlation Functions Using RPA

RPA for our field theory essentially consists of an expansion of the effective energy with respect to the external fields W and U around the saddle point solution of the system. Because we are regarding systems with temperatures above the ODT, the saddle point approximation will result in a completely disordered phase. To derive the full expansion of E_0 to second order of δU and δW, we start off by expanding the single chain partition function Q. Using the microscopic densities $\hat{\phi}_{A/B,1}$ of A- and B-monomers of a single polymer chain, we may rewrite $Q[U,W]$ in the following way:

$$Q[U,W] = \int \mathscr{D}\{\mathbf{r}_A\}\ \mathscr{D}\{\mathbf{r}_B\}\ \mathscr{P}_A[\mathbf{r}_A]\ \mathscr{P}_B[\mathbf{r}_B] \times \exp\left[-\frac{\rho}{N}\int_V \mathrm{d}^3\mathbf{r}\ \{(U(\mathbf{r}) + W(\mathbf{r}))\hat{\phi}_{A,1}(\mathbf{r}) + (U(\mathbf{r}) - W(\mathbf{r}))\hat{\phi}_{B,1}(\mathbf{r})\}\right] \quad (48)$$

Using the definitions $\phi = \hat{\phi}_{A,1} - \hat{\phi}_{B,\,1}$ and $\xi = \hat{\phi}_{A,1} + \hat{\phi}_{B,1}$, Q has the form

$$Q[U,W] = \int \mathscr{D}\{\mathbf{r}_A\}\ \mathscr{D}\{\mathbf{r}_B\}\ \mathscr{P}_A[\mathbf{r}_A]\ \mathscr{P}_B[\mathbf{r}_B] \times \exp\left[-\frac{\rho}{N}\int_V \mathrm{d}^3\mathbf{r}\ \{U(\mathbf{r})\ \xi(\mathbf{r}) + W(\mathbf{r})\ \phi(\mathbf{r})\}\right] \quad (49)$$

Now we expand Q as a function of $W = \langle W\rangle_0 + \delta W$, $U = \langle U\rangle_0 + \delta U$, $\phi = \langle\phi\rangle_0 + \delta\phi$, and $\xi = \langle\xi\rangle_0 + \delta\xi$. Above the ODT $\langle W\rangle_0$ and $\langle U\rangle_0$ are spatially independent constants, $\langle\xi\rangle_0 = 1$ and $\langle\phi\rangle_0 = 2f - 1$. Using the Fourier transforms of all the quantities, we may write the partition function as

$$Q[\delta U,\delta W] = \exp[-\langle U\rangle_0 - \langle W\rangle_0(2f-1)]\int \mathscr{D}\{\mathbf{r}_A\}\ \mathscr{D}\{\mathbf{r}_B\}\ \mathscr{P}_A[\mathbf{r}_A]\ \mathscr{P}_B[\mathbf{r}_B] \exp\left[-\frac{\rho}{N}\frac{1}{8\pi^3}\int \mathrm{d}^3\mathbf{q}\ \{\delta U(\mathbf{q})\delta\xi(-\mathbf{q}) + \delta W(\mathbf{q})\delta\phi(-\mathbf{q})\}\right] \quad (50)$$

If the fluctuations of the densities and the fields are weak, the exponential function may be expanded:

$$Q[\delta U,\delta W] = \exp[-\langle U\rangle_0 - \langle W\rangle_0(2f-1)] \int \mathscr{D}\{\mathbf{r}_A\}\ \mathscr{D}\{\mathbf{r}_B\}\ \mathscr{P}_A[\mathbf{r}_A]\ \mathscr{P}_B[\mathbf{r}_B] \left\{1 - \frac{1}{8\pi^3}\frac{\rho}{N}\int \mathrm{d}^3\mathbf{q}\ \{\delta U(\mathbf{q}) \times \delta\xi(-\mathbf{q}) + \delta W(\mathbf{q})\delta\phi(-\mathbf{q})\} + \frac{1}{2}\frac{1}{(8\pi^3)^2}\left(\frac{\rho}{N}\right)^2 \int \mathrm{d}^3\mathbf{q} \int \mathrm{d}^3\mathbf{q}'\ \{\delta U(\mathbf{q})\delta U(\mathbf{q}')\delta\xi(-\mathbf{q})\delta\xi(-\mathbf{q}') + 2\delta U(\mathbf{q})\delta W(\mathbf{q}') \times \delta\xi(-\mathbf{q})\delta\phi(-\mathbf{q}') + \delta W(\mathbf{q})\delta W(\mathbf{q}')\delta\phi(-\mathbf{q})\delta\phi(-\mathbf{q}')\}\right\} \quad (51)$$

$$= \exp[-\langle U\rangle_0 - \langle W\rangle_0(2f-1)]Q_0\left\{1 - \left\langle\frac{1}{8\pi^3}\frac{\rho}{N}\int \mathrm{d}^3\mathbf{q}\ \{\delta U(\mathbf{q})\delta\xi(-\mathbf{q}) + \delta W(\mathbf{q})\delta\phi(-\mathbf{q})\} + \frac{1}{2}\frac{1}{(8\pi^3)^2}\left(\frac{\rho}{N}\right)^2 \int \mathrm{d}^3\mathbf{q} \int \mathrm{d}^3\mathbf{q}'\ \{\delta U(\mathbf{q})\delta U(\mathbf{q}') \times \delta\xi(-\mathbf{q})\delta\xi(-\mathbf{q}') + 2\delta U(\mathbf{q})\delta W(\mathbf{q}')\delta\xi(-\mathbf{q})\delta\phi(-\mathbf{q}') + \delta W(\mathbf{q})\delta W(\mathbf{q}')\delta\phi(-\mathbf{q})\delta\phi(-\mathbf{q}')\}\right\rangle_{\mathrm{nf}}\right\} \quad (52)$$

$$= \exp[-\langle U\rangle_0 - \langle W\rangle_0(2f-1)]Q_0\left\{1 - \frac{\rho}{N}\int \mathrm{d}^3\mathbf{q}\ \{\delta U(\mathbf{q})\langle\delta\xi(-\mathbf{q})\rangle_{\mathrm{nf}} + \delta W(\mathbf{q})\langle\delta\phi(-\mathbf{q})\rangle_{\mathrm{nf}}\} + \frac{1}{2}\frac{1}{(8\pi^3)^2}\left(\frac{\rho}{N}\right)^2 \int \mathrm{d}^3\mathbf{q} \int \mathrm{d}^3\mathbf{q}\ \{\delta U(\mathbf{q})\delta U(\mathbf{q}') \times \langle\delta\xi(-\mathbf{q})\delta\xi(-\mathbf{q}')\rangle_{\mathrm{nf}} + 2\delta U(\mathbf{q})\delta W(\mathbf{q}')\langle\delta\xi(-\mathbf{q})\delta\phi(-\mathbf{q}')\rangle_{\mathrm{nf}} + \delta W(\mathbf{q})\delta W(\mathbf{q}')\langle\delta\phi(-\mathbf{q})\delta\phi(-\mathbf{q}')\rangle_{\mathrm{nf}}\}\right\} \quad (53)$$

Q_0 is the partition function of a single Gaussian polymer chain in an environment where no external field is present. $\langle\ \rangle_{\mathrm{nf}}$ expresses the average if no external field is acting on the polymer. The average changes of the densities $\langle\delta\phi\rangle_{\mathrm{nf}}$ and $\langle\delta\xi\rangle_{\mathrm{nf}}$ vanish. For the single-chain correlation functions we use the results derived by Leibler:

$$\langle\delta\xi(-\mathbf{q})\delta\xi(-\mathbf{q}')\rangle_{\mathrm{nf}} = \langle\delta\phi_A(-\mathbf{q})\delta\phi_A(-\mathbf{q}')\rangle_{\mathrm{nf}} + 2\langle\delta\phi_A(-\mathbf{q})\delta\phi_B(-\mathbf{q}')\rangle_{\mathrm{nf}} + \langle\delta\phi_B(-\mathbf{q})\delta\phi_B(-\mathbf{q}')\rangle_{\mathrm{nf}} \quad (54)$$

$$= 8\pi^3\delta(\mathbf{q} - \mathbf{q}')[S_{AA}(q) + 2S_{AB}(q) + S_{BB}(q)] \quad (55)$$

$$\langle\delta\xi(-\mathbf{q})\delta\phi(-\mathbf{q}')\rangle_{\mathrm{nf}} = \langle\delta\phi_A(-\mathbf{q})\delta\phi_A(-\mathbf{q}')\rangle_{\mathrm{nf}} - \langle\delta\phi_B(-\mathbf{q})\delta\phi_B(-\mathbf{q}')\rangle_{\mathrm{nf}} \quad (56)$$

$$= 8\pi^3\delta(\mathbf{q} - \mathbf{q}')[S_{AA}(q) - S_{BB}(q)] \quad (57)$$

$$\langle\delta\phi(-\mathbf{q})\delta\phi(-\mathbf{q}')\rangle_{\mathrm{nf}} = \langle\delta\phi_A(-\mathbf{q})\delta\phi_A(-\mathbf{q}')\rangle_{\mathrm{nf}} - 2\langle\delta\phi_A(-\mathbf{q})\delta\phi_B(-\mathbf{q}')\rangle_{\mathrm{nf}} + \langle\delta\phi_B(-\mathbf{q})\delta\phi_B(-\mathbf{q}')\rangle_{\mathrm{nf}} \quad (58)$$

$$= 8\pi^3\delta(\mathbf{q} - \mathbf{q}')[S_{AA}(q) - 2S_{AB}(q) + S_{BB}(q)] \quad (59)$$

with the single-chain correlation functions $S_{AA}(q)$, $S_{AB}(q)$, and $S_{BB}(q)$ from eqs 29−31. Finally, we may rewrite Q as

$$Q = \exp[-\langle U\rangle_0 - \langle W\rangle_0(2f-1)]Q_0 \exp\left[\frac{1}{2}\frac{1}{8\pi^3}\left(\frac{\rho}{N}\right)^2\int \mathrm{d}^3\mathbf{q}\,\{\delta U(\mathbf{q})\delta U(\mathbf{q})(S_{AA}(q)+2S_{AB}(q)+S_{BB}(q)) + 2\delta U(\mathbf{q})\delta W(\mathbf{q})(S_{AA}(q)-S_{BB}(q)) + \delta W(\mathbf{q})\delta W(\mathbf{q})(S_{AA}(q)-2S_{AB}(q)+S_{BB}(q))\}\right] \quad (60)$$

Inserting this single-chain partition function the expansion of the energy E_0 of eq 18 around the saddle point solution leads to

$$E_0 = \frac{\rho}{N}\int_V \mathrm{d}^3\mathbf{r}\left\{\frac{\chi N}{4} - \langle U\rangle_0 + \frac{1}{\chi N}\langle W\rangle_0^2\right\} - \ln Q_0 + \frac{1}{2}\left(\frac{\rho}{N}\right)^2\int \mathrm{d}^3\mathbf{q}\left\{\delta W(q)\delta W(-q)\left[\frac{N}{\rho}\frac{2}{\chi N} - (S_{AA}(q) - 2S_{AB}(q) + S_{BB}(q))\right] - 2\delta W(q)\delta U(-q)[S_{AA}(q) - S_{BB}(q)] - \delta U(q)\delta U(-q)[(S_{AA}(q) + 2S_{AB}(q) + S_{BB}(q))]\right\} \quad (61)$$

$$= \frac{\rho}{N}\int_V \mathrm{d}^3\mathbf{r}\left\{\frac{\chi N}{4} - \langle U\rangle_0 + \frac{1}{\chi N}\langle W\rangle_0^2\right\} - \ln Q_0 + \frac{1}{2}\left(\frac{\rho}{N}\right)^2\int \mathrm{d}^3\mathbf{q}\,\{C_{\mathrm{WW}}(q)\delta W(q)\delta W(-q) + 2C_{\mathrm{UW}}(q)\delta W(q)\delta U(-q) + C_{\mathrm{UU}}(q)\delta U(q)\delta U(-q)\} \quad (62)$$

From this energy we can easily identify the correlation functions we were looking for. They are given by eqs 22−28.

References and Notes

(1) Alexandre, M.; Dubois, P. *Mater. Sci. Eng. Rev.* **2000**, *28*, 1.
(2) Schmidt, D.; Shah, D.; Giannelis, E. *Curr. Opin. Solid State Mater. Sci.* **2002**, *6*, 205.
(3) Black, C.; Murray, C.; Sandstrom, R.; Sun, S. *Science* **2000**, *290*, 1131.
(4) Mayer, A.; Mark, J. *J. Polym. Sci., Part A: Polym. Chem.* **1997**, *35*, 3151.
(5) Sevink, G.; Zvelindovsky, A.; van Flimmeren, B.; Maurits, N.; Fraaije, J. *J. Chem. Phys.* **1999**, *110*, 2250.
(6) Ginzburg, V.; Gibbons, C.; Qiu, F.; Peng, G.; Balazs, A. *Macromolecules* **2000**, *33*, 6140.
(7) Ginzburg, V.; Qiu, F.; Balazs, A. *Polymer* **2002**, *43*, 461.
(8) Huh, J.; Ginzburg, V.; Balazs, A. *Macromolecules* **2000**, *33*, 8085.
(9) Wang, Q.; Nealy, P.; de Pablo, J. *J. Chem. Phys.* **2003**, *118*, 11278.
(10) Thompson, R.; Ginzburg, V.; Matsen, M.; Balazs, A. *Macromolecules* **2002**, *35*, 1060.
(11) Ginzburg, V.; Singh, C.; Balazs, A. *Macromolecules* **2000**, *33*, 1089.
(12) Ginzburg, V.; Balazs, A. *Adv. Mater.* **2000**, *12*, 1805.
(13) Groenewold, J.; Fredrickson, G. *Eur. Phys. J. E* **2001**, *5*, 171.
(14) Chatterjee, A.; Schweizer, K. *J. Chem. Phys.* **1998**, *109*, 10464.
(15) Chatterjee, A.; Schweizer, K. *Macromolecules* **1999**, *32*, 923.
(16) Fredrickson, G.; Ganesan, V.; Drolet, F. *Macromolecules* **2002**, *35*, 16.
(17) Tarazona, P. *Mol. Phys.* **1984**, *52*, 81.
(18) Carnahan, N.; Starling, K. *J. Chem. Phys.* **1969**, *51*, 635.
(19) Matsen, M.; Schick, M. *Phys. Rev. Lett.* **1994**, *72*, 2660.
(20) Leibler, L. *Macromolecules* **1980**, *13*, 1602.
(21) Shi, A.-C.; Noolandi, J.; Desai, R. *Macromolecules* **1996**, *29*, 6487.
(22) Helfand, E. *J. Chem. Phys.* **1975**, *62*, 999.
(23) Feynman, R.; Hibbs, A. *Quantum Mechanics and Path Integrals*; McGraw-Hill Book Co.: New York, 1965.
(24) Rasmussen, K.; Kalosakas, G. *J. Polym. Sci., Part B: Polym. Phys.* **2002**, *40*, 1777.
(25) Drolet, F.; Fredrickson, G. *Phys. Rev. Lett.* **1999**, *83*, 4317.
(26) Sides, S.; Fredrickson, G. *Polymer* **2003**, *44*, 5859.

MA035849P